Original Paper

Multivariate natural gas price forecasting model with feature selection, machine learning and chernobyl disaster optimizer

Pei Du [a], Xuan-Kai Zhang [a], Jun-Tao Du [b,*], Jian-Zhou Wang [c]

[a] *School of Business, Jiangnan University, Wuxi, 214122, Jiangsu, China*
[b] *School of Statistics & Applied Mathematics, Anhui University of Finance and Economics, Bengbu, 233030, Anhui, China*
[c] *Institute of Systems Engineering, Macau University of Science and Technology, Macau SAR, 999078, China*

A R T I C L E I N F O

Article history:
Received 23 December 2024
Received in revised form
18 September 2025
Accepted 19 September 2025
Available online 24 September 2025

Edited by Jia-Jia Fei

Keywords:
Natural gas price forecasting
Multivariate forecasting model
Machine learning
Chernobyl disaster optimizer

A B S T R A C T

The significance of accurately forecasting natural gas prices is far-reaching and significant, not only for the stable operation of the energy market, but also as a key element in promoting sustainable development and addressing environmental challenges. However, natural gas prices are affected by multiple source factors, presenting complex, unstable nonlinear characteristics hindering the improvement of the prediction accuracy of existing models. To address this issue, this study proposes an innovative multivariate combined forecasting model for natural gas prices. Initially, the study meticulously identifies and introduces 16 variables impacting natural gas prices across five crucial dimensions: the

factors such as supply and demand, exchange rates, macroeconomic policies, extreme weather, wars, and environmental conditions (Shi and Shen, 2021; Li et al., 2021; Zheng et al., 2023). Specifically, long-term trends in natural gas prices are driven by supply and demand, with natural gas inventory levels, production, imports and exports, and consumption having a significant impact on prices (Xia and Li, 2024; Yarlagadda et al., 2024). Temperatures are also correlated with natural gas consumption, which indirectly affects natural gas prices (Li et al., 2022). The impact of the price linkage effect of alternative energy sources, such as crude oil as a core substitute, whose price volatility directly affects natural gas pricing (Perifanis and Dagoumas, 2021). Geopolitical risks, such as the Russia-Ukraine conflict, affect gas prices by triggering price volatility through supply chain disruptions, export restrictions and investment uncertainty (Iliyasu et al., 2025). In addition, exchange rate fluctuations (e.g., EUR/USD, USD/JPY) can also have a nonlinear impact on gas prices due to the cross-border nature of trading gas futures. Therefore, the complex characteristics of natural gas prices and their intricacies pose a great challenge to forecasting natural gas prices accurately.

1.2. Literature review

1.2.1. Linear and nonlinear forecasting models

The linear forecasting model, such as autoregressive moving average (ARMA) model (Ervural et al., 2016), typically rely on assumptions about the statistical distribution and stationarity of the research data, and are unable to capture the nonlinear characteristics of energy prices, resulting in high prediction errors (Gao et al., 2023). However, natural gas price series often exhibit complex nonlinear characteristics, so it is necessary to introduce nonlinear models to improve prediction performance (Xie et al., 2023). For example, Malliaris and Malliaris (2008) utilized linear and nonlinear models to predict energy product prices, finding that nonlinear models yielded lower prediction errors than linear models. Therefore, nonlinear models, particularly artificial intelligence (AI) models such as artificial neural networks (ANNs) (Yang et al., 2023a), support vector regression (SVR) (Xian and Che, 2022), and deep learning models, have become increasingly popular for gas price prediction (Sun et al., 2021), because they can handle nonlinear relationships and achieve high prediction accuracy. Zheng et al. (2023) established an optimized SVR to predict gas price, ultimately validating that nonlinear models outperform linear models in terms of nonlinear fitting capability. However, AI models still face some challenges that need to be addressed, such as overfitting, slow convergence, and local optima, etc. (Niu et al., 2020).

1.2.2. Univariate and multivariate forecasting models

Recently, AI models have been widely applied to energy price forecasting. However, in addition to selecting the appropriate model, whether to adopt a multivariate analysis method remains an issue in this field. Wang et al. (2021) obtained excellent forecasting results using a univariate AI model, but this model was designed for short-term prediction. In general, previous findings have shown that univariate approaches perform satisfactorily in most cases, but their prediction performance tends to be significantly degraded when dealing with long-term prediction tasks and large data fluctuations (Cabello-López et al., 2023; Ziel and Weron, 2018). Meanwhile, more and more researchers and scholars have confirmed that various factors contribute to fluctuations in natural gas prices, such as requirement, prices of other energy products, extreme weather, and geopolitical events, etc. However, existing studies tend to focus on univariate forecasting approaches, which are difficult to effectively capture these complex patterns behind them and deal with the effects of multiple factors (Ziel and Weron, 2018). Therefore, it is crucial and meaningful to construct a multivariate natural gas forecasting model that considers relevant influencing factors. To our knowledge, only a limited number of studies have developed multivariate natural gas price forecasting models and achieved a certain degree of improvement in accuracy (Su et al., 2019; Guan et al., 2022; Li et al., 2021; Zheng et al., 2023). However, these researches only introduced multivariate models and did not compare them with univariate models. Thus, drawing on experience from other energy market studies, it is necessary to simultaneously develop both univariate and multivariate methods and further explore the impact of multivariate models on the accuracy through comparison (Ziel and Weron, 2018).

1.2.3. Individual, hybrid and combined models

Individual models are simple models based on different prediction principles that achieve prediction by modeling historical data sequences (Wang et al., 2017). However, researchers have progressively confirmed that each model has its own strengths and weaknesses, with no single model inherently superior to others (Guo et al., 2011). Especially considering the uncertainty, dynamism, and nonlinear characteristics exhibited by energy prices (Du et al., 2018), a single model struggles to effectively capture specific patterns within the data and achieve accurate predictions (Niu et al., 2022). As a result, hybrid forecasting models and combined forecasting models have emerged (Hao et al., 2023). Hybrid models have become a leading approach in energy price forecasting, combining data preprocessing, predictive methods, optimization techniques, and feature selection to enhance accuracy. They have been applied in time series prediction across diverse domains (Niu and Wang, 2019; Jiang et al., 2023; Wu et al., 2022). For instance, Lin et al. (2022) v natural gas price forecasting models without comparing univariate and multivariate forecasting results. Meanwhile, the neglect of the importance of data on influencing factors may lead to insufficient forecasting accuracy.

Comment 3: Existing research on energy price forecasting indicates that individual models struggle to meet accuracy requirements, and hybrid models based on single models and multiple techniques or combined models using different forecasting models have significant prediction superiority and have become the mainstream research paradigm for energy price prediction. However, most existing literature relies on single-strategy approaches, with limited in-depth exploration of hybrid or combined strategies.

1.3. Innovations and main contributions

According to the analysis and summary of existing literature, this study conducts comparative analyses from multiple perspectives, such as feature selection, univariate and multivariate models, single models, hybrid models and combined models, respectively, to explore their impact on the performance of natural gas price prediction. And finally it proposes an improved combined multivariate forecasting model, which can provide a reference to the prediction and decision-making of natural gas price. This research offers the following innovations and contributions:

(1) **Proposing a novel combined model with high accuracy and stability.** An improved combined multivariate forecasting model is developed for natural gas price prediction. It combines feature selection (FS) algorithms, Chernobyl disaster optimizer (CDO) and machine learning techniques, including a hybrid model of convolutional neural network (CNN) and long short-term memory (LSTM), i.e., CNN-LSTM and SVR, namely FS-CDO-CNN-LSTM&SVR model. In comparison to the conventional univariate and multivariate models, the developed combined model can demonstrate higher prediction accuracy and stronger prediction stability.

(2) **Comprehensive consideration and analysis of multi-source influencing factors.** The combined multivariate forecasting model proposed in this study integrates sixteen multi-source influences on natural gas prices, including five dimensions: production, marketing, commodities, political and economic indicators of the United States (U.S.) and temperature. In order to clarify which variable datasets are more effective, three different types of feature selection algorithms are introduced to screen features of the influencing variables to further enhance the performance of natural gas price prediction.

(3) **Scientific and effective validation of model performance.** Three comparison experiments are designed. Moreover, six univariate prediction comparison models, thirteen multivariate prediction comparison models, involving linear and nonlinear models, single, hybrid and combined models, while several model evaluation criteria, hypothesis testing, stability testing, and improvement ratio from the proposed model are introduced to comprehensively validate the presented combined method. And the final results demonstrate that the combined forecasting method presented in this work has a significant improvement of performance in natural gas price prediction.

The remaining sections of this study are arranged as below. The second section introduces the research framework

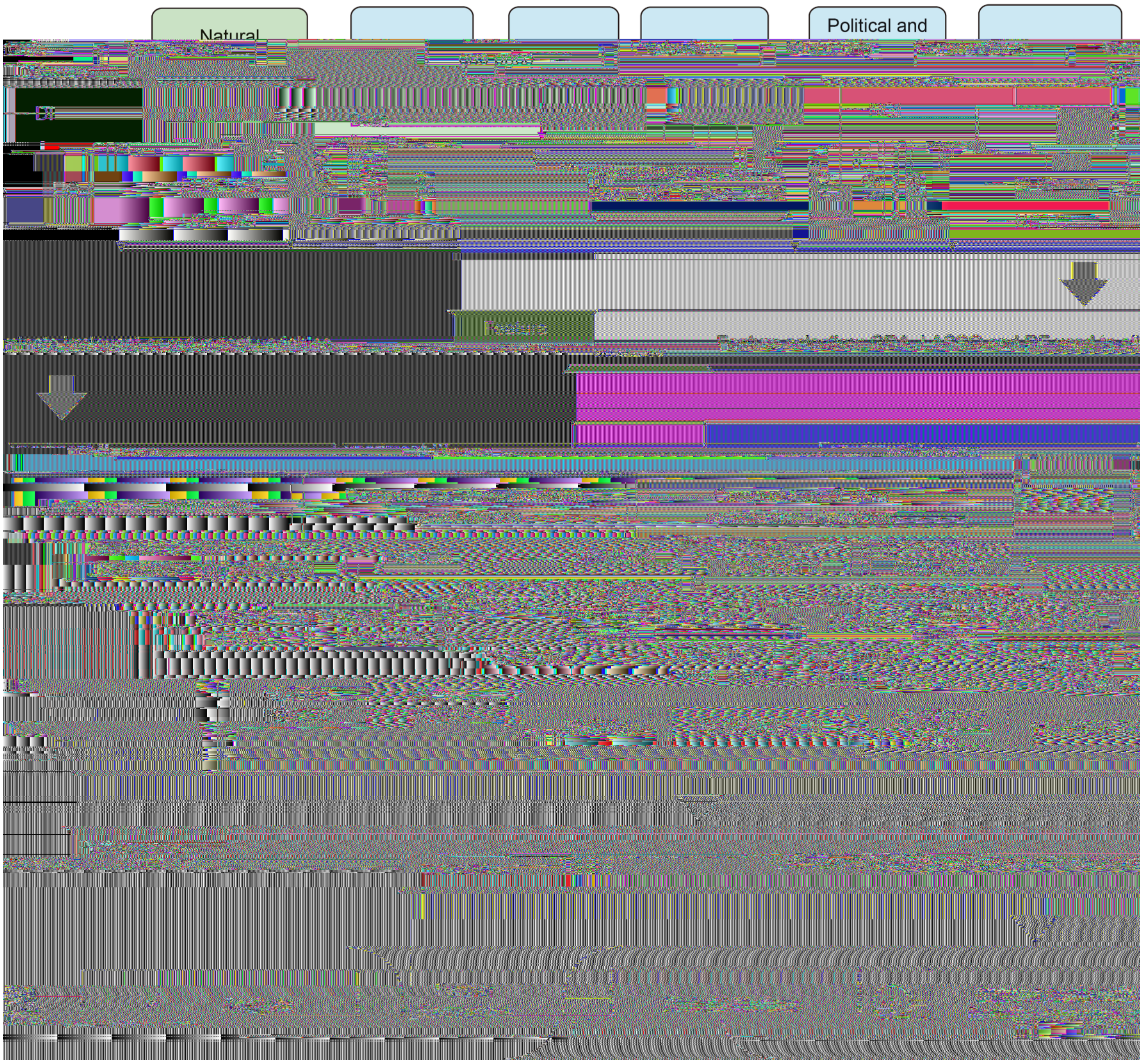

Fig. 1. The research framework of this study.

function serves to contract the original coefficients, causing the coefficients of unimportant variables to be diminished to zero. This effectively eliminates the impact of irrelevant variables on the model's predictive performance. The parameter is estimated using the following formula:

$$\widehat{\beta}_{\text{Lasso}} = \operatorname{argmin}\left\| y - \sum_{i=1}^{n} x_i \beta_i \right\|^2 + \lambda \sum_{i=1}^{n} |\beta_i| \tag{1}$$

where the penalty parameter λ determines the model's complexity. As λ increases, the linear model's feature variables face a greater penalty. For further details on LASSO, refer to (Kapoor and Wichitaksorn, 2023; Mishra et al., 2021; Tian et al., 2023).

3.1.2. *Grey relation analysis (GRA)*

GRA method is a method used to measure the degree of similarity or dissimilarity in the development trends between the target variable and its factors. The higher the correlation, the stronger the relationship with the target variable and the more significant the impact on the target variable. The detailed mathematical formulas are as follows (Guo et al., 2022; Liu and Yu, 2007).

$$\begin{cases} \theta_i = \dfrac{1}{n} \displaystyle\sum_{k=1}^{n} \zeta_i(k) \\ \zeta_i(k) = \dfrac{\min\limits_j \min\limits_l |x_0(l) - x_j(l)| + \gamma \max\limits_j \max\limits_l |x_0(l) - x_j(l)|}{|x_0(k) - x_i(k)| + \gamma \max\limits_j \max\limits_l |x_0(l) - x_j(l)|} \end{cases} \tag{2}$$

where θ_i represents the grey relation degree between the i-th factor and the target variable, and $\zeta_i(k)$ represents that of the i-th factor at the k-th moment. $\min\limits_j \min\limits_l |x_0(l) - x_j(l)|$ is the global minimum absolute difference between the target variable and all factors across all moments, and $\max\limits_j \max\limits_l |x_0(l) - x_j(l)|$ is the maximum. $\gamma \in [0, 1]$ represents recognition coefficient, generally set $\gamma = 0.5$.

3.1.3. *Random forest (RF)*

During feature selecting, RF uses bootstrap aggregating to build each decision tree (Breiman, 2001). Firstly, RF uses the Bootstrap sampling method to randomly draw samples from the original dataset. This process allows some samples to appear multiple times in a single decision tree, while others may be excluded. For each decision tree's construction, RF randomly selects k features from the dataset as candidate features, limiting the splitting process to these k features. Typically, the value of k is set to the square root of the total number of features or a fraction of n, where n represents the total number of features.

RF algorithm has been successfully utilized for load forecasting (Fan et al., 2022), wave height forecasting (Ali et al., 2023), solar radiation energy (Prasad et al., 2019) and stock market forecasting (Park et al., 2022). Additionally, the detailed theoretical descriptions of RF can be found in the literature (Biau, 2012; Zhang et al., 2021; Behrens et al., 2018).

3.2. Chernobyl disaster optimizer (CDO)

The CDO algorithm (Shehadeh, 2023) is derived from the Chernobyl nuclear reactor core explosion. In this algorithm, nuclear explosions emit different kinds of radiation due to nuclear instability. The most common types of radiation include α, β and γ particles. CDO primarily concentrates on the updating methods of three types of particles. α, β and γ will pose a threat to humans. These particles will travel away from the reactor's core (a high-pressure area) towards regions where humans are located (low-pressure areas), ultimately leading to disaster. CDO assumes that the victims (humans) are moving as these particles attack them. Based on the estimation, the following equation simulates the process of speed decreasing to 0, where WS_{h} refers the walking speed of human (0–3 miles/h).

$$WS_{\mathrm{h}} = 3 - 1 \times (3/\mathrm{Maximum\_Iteration}) \tag{3}$$

The gradient descent factors for the three particles when attacking humans is shown in Eq. (4).

$$\begin{cases} v_\gamma = \left(X_\gamma(t) - \rho_\gamma \times \Delta_\gamma\right) \\ v_\beta = 0.5 \times \left(X_\beta(t) - \rho_\beta \times \Delta_\beta\right) \\ v_\alpha = 0.25 \times \left(X_\alpha(t) - \rho_\alpha \times \Delta_\alpha\right) \end{cases} \tag{4}$$

where $X_i(t), i = \gamma, \beta, \alpha$ represents the current position of gamma, beta and alpha particles; $\rho_i, i = \gamma, \beta, \alpha$ is the propagation of gamma, beta and alpha particles; $\Delta_i, i = \gamma, \beta, \alpha$ is the difference between human positions and positions of gamma, beta and alpha particles.

By Eq. (5), the $\rho_i, i = \gamma, \beta, \alpha$ can be calculated.

$$\begin{cases} \rho_\gamma = \dfrac{X_{\mathrm{h}}}{S_\gamma} - (WS_{\mathrm{h}} \times \mathrm{rand}()) \\ \rho_\beta = \dfrac{X_{\mathrm{h}}}{0.5 \times S_\beta} - (WS_{\mathrm{h}} \times \mathrm{rand}()) \\ \rho_\alpha = \dfrac{X_{\mathrm{h}}}{0.25 \times S_\alpha} - (WS_{\mathrm{h}} \times \mathrm{rand}()) \end{cases} \tag{5}$$

where X_{h} refers to the area in which humans are walking, represented as the area of a circle, which can be computed using Eq. (6), The speed of the particle, denoted as $S_i, i = \gamma, \beta, \alpha$, can randomly range from 1 to 300,000, with specific values such as 270,000 and 16,000 km/s, as shown in Table 1. To standardize this value, we apply the logarithmic transformation, as given in Eq. (6).

Table 1
Parameters of the CDO algorithm.

Radiation type	Speed of particle ($S_{\text{type of particle}}$), km/s
Alpha (α)	16,000
Beta (β)	270,000
Gamma (γ)	300,000

$$X_{\mathrm{h}} = r^2 \times \pi \tag{6}$$

in which r is a random value within (0, 1).

$$\begin{cases} S_\gamma = \log\left(\mathrm{rand}(1:300000\right) \\ S_\beta = \log\left(\mathrm{rand}(1:270000\right) \\ S_\alpha = \log\left(\mathrm{rand}(1:16000\right) \end{cases} \tag{7}$$

The $\Delta_i, i = \gamma, \beta, \alpha$ is the different from γ, β, α, and related positions are calculated using Eq. (8).

$$\Delta_i = |A_i \times X_i(t) - X_{\mathrm{T}}(t)|, i = \gamma, \beta, \alpha \tag{8}$$

where $X_{\mathrm{T}}(t)$ denotes the averages of whole positions, $A_i, i = \gamma, \beta, \alpha$ refers to the area over which these particles (γ, β, α), represented as the area of a circle, and is calculated using Eq. (9).

$$A_i = r^2 \times \pi, i = \gamma, \beta, \alpha \tag{9}$$

in which r is a random value within (0, 1).

On the basis of the *Galileo Galilei* equations of motion, the mean of total speed of γ, β and α can be taken through the following formula.

$$X_{\mathrm{T}} = \frac{(v_\alpha + v_\beta + v_\gamma)}{3} \tag{10}$$

3.3. Forecasting models

The forecasting models employed in this study are described in detail as follows.

3.3.1. Long short-term memory (LSTM)

As a specialized form of recurrent neural network (RNN), LSTM (Hochreiter and Schmidhuber, 1997) can efficiently regulate information flow by introducing a gating mechanism, enabling it to better handle long-term dependencies. It stores and transmits information through unit states, which are designed to allow LSTM to retain long-term information without losing important details due to prolonged intervals. An LSTM unit consists of three gates: the input gate i_t, the forget gate f_t, and the output gate o_t.

Input gate:

$$i_t = \sigma(W_i[h_{t-1}, x_t] + b_i) \tag{11}$$

Forget gate:

$$f_t = \sigma(W_t[h_{t-1}, x_t] + b_t) \tag{12}$$

Output gate:

$$o_t = \sigma(W_o[h_{t-1}, x_t] + b_o) \tag{13}$$

Cell state:

$$\begin{cases} C_t = f_t \otimes C_{t-1} + i_t \otimes \tilde{C}_t \\ \tilde{C}_t = \tanh(W_C[h_{t-1}, x_t] + b_C) \end{cases} \tag{14}$$

Output vector:

$$h_t = o_t \otimes \tanh(C_t) \tag{15}$$

where x_t is input time series, $\otimes$ represents the dot product; h_{t-1} denotes previous output; C_{t-1}, C_t and $\tilde{C}_t$ are the previous memory state, current state and intermediate state, respectively.

3.3.2. Convolutional neural networks (CNN)

CNN is a type of deep feed-forward neural network that offers advantages like local connections and weight sharing, which has achieved notable success in tasks. In this research, CNN is incorporated to boost the prediction accuracy of LSTM, using a one-dimensional convolution approach (Yao et al., 2023). And the related equations are shown as below.

$$Y = \sigma(\boldsymbol{W} * X + b) \tag{16}$$

in which Y is the extracted features; $\boldsymbol{W}$ is the weight matrix; X indicates the input data; b and ρ are bias vector and sigmoid function, respectively.

3.3.3. Support vector regression (SVR)

The core idea of SVR is to create a hyperplane in the feature space that maximizes the margin between the training data points and the hyperplane. To perform regression prediction, SVR introduces a notion of slack variables to allow for a certain degree of error tolerance. The goal of SVR is to reduce the complexity of the model while simultaneously reducing forecast inaccuracy and enlarging the margin (Chapelle et al., 1999).

Given training time series $\{(x_i, y_i)\}_i^n$, thereinto x_i is the input features, n denotes the length of the training time series and y_i represents the corresponding output value. The regression method can be built for the high-dimensional feature space expressed as following equation:

$$f(x) = \boldsymbol{\omega} * \Psi(x) + \upsilon \tag{17}$$

where $\psi(x)$ represents the nonlinear mapping from the input space to the high-dimensional space, $\boldsymbol{\omega}$ is the weight vector, and ν is the threshold value.

$$R(f) = C\frac{1}{n}\sum_{i=1}^{n} L\ (y_i, f(x_i)) + \frac{1}{2}\|w\|^2 \tag{18}$$

where L () represents loss function, C is the penalty parameter, represents tube size. Then Eq. (17) can be transformed into the following equation using two slack variables δ and δ^*:

$$\min \frac{1}{2}\|w\|^2 + C\sum_{i=1}^{n}(\delta_i + \delta_i^*)$$
$$s.t. \begin{cases} y_{\boldsymbol{i}} - \omega_i * \varphi(x_i) - b_i \le \quad + \delta_i \\ w_i * \varphi(x_i) + b - y_{\boldsymbol{i}} \le \quad + \delta_i^* \\ \delta_i + \delta_i^* \ge 0, i = 1, 2, \dots, n \end{cases} \tag{19}$$

Thus, the dual form can be presented as the following equation:

$$\max -\frac{1}{2}\sum_{i=1}^{n}\sum_{j=1}^{n}(\alpha_i - \alpha_i^*)\left(\alpha_j - \alpha_j^*\right)K\left(x_i, x_j\right) - \cdot \sum_{i=1}^{n}(\alpha_i + \alpha_i^*) + \sum_{i=1}^{n}(\alpha_i - \alpha_i^*)$$
$$s.t. \begin{cases} \sum_{i=1}^{n}(\alpha_i - \alpha_i^*) = 0 \\ 0 \le \alpha_i \le C, i = 1, 2, \dots, n \\ 0 \le \alpha_i^* \le C, i = 1, 2, \dots, n \end{cases} \tag{20}$$

where α_i and α_i^* are Lagrange multipliers. $K(x_i, x_j) = <\varphi(x_i)\varphi(x_j)>$ represents the kernel function, which can be written as:

$$K\left(x_i, x_j\right) = \exp\left(-\frac{\|x_i - x_j\|^2}{2\sigma}\right) = \exp\left(-\theta\|x_i - x_j\|^2\right) \tag{21}$$

where σ denotes the width of the radial basis function. The nonlinear regression function is shown in Eq. (22).

$$f(x) = \sum_{i=1}^{n}(\alpha_i - \alpha_i^*)K\left(x_i, x_j\right) + b \tag{22}$$

3.4. The proposed combined model

Considering that both CNN-LSTM optimized by CDO algorithm (CDO-CNN-LSTM) and SVR perform well in the work, this study employs an adaptive weighting module (AWM), which can be used for parallel prediction using multiple models by assigning weight values to individual models, and ultimately constructs a more accurate prediction model. Firstly, the time series are inputted into the model, the results of CDO-CNN-LSTM and SVR can be obtained respectively, which are inputted into their respective thick layers and assigned different weight values by the AWM, and then the outputs of CDO-CNN-LSTM and SVR are linearly summed with the weights to construct the proposed combined model (CDO-CNN-LSTM&SVR). Finally, the forecasting values can be obtained using the following equation:

$$\widehat{y} = \boldsymbol{\theta}_1\widehat{y}_{M_1} + \boldsymbol{\theta}_2\widehat{y}_{M_2} \tag{23}$$

where $\widehat{y}_{M_1}$ and $\widehat{y}_{M_2}$ are the forecasting values of CDO-CNN-LSTM and SVR, respectively. $\boldsymbol{\theta}_1$, $\boldsymbol{\theta}_2$ are the corresponding weight matrices, $\widehat{y}$ is the output value of the added layer.

To dynamically evaluate model accuracy on sample data, AWM uses the following equation during the training process to find optimal weights:

$$APE = \left|\frac{\widehat{y}_t - y_t}{y_t}\right| \tag{24}$$

APE indicates the absolute percentage error of the fitted and actual values, y_t and $\widehat{y}_t$ are the t-th observed and forecasting values, respectively. The combined model involves multiple stages, so it is necessary to analyze its complexity. The following is an asymptotic analysis of each stage of the combined model, which can be used as a reference for evaluating training time and hardware consumption.

Feature selection and CDO optimization: CDO for hyper-parameter tuning operates with a complexity of O(Iterations $\times$

Population_Size $\times$ $(O_{SVR} + O_{LSTM}))$, where $O_{LSTM} \approx O(\text{num\_epochs} \times \text{time\_steps} \times \text{hidden\_nodes}^2)$ and $O_{SVR} \approx O(n^3)$ (kernel matrix inversion) dominate the cost (Shi et al., 2024).

CNN-LSTM: Spatial-temporal modeling via Conv-Former and stacked LSTM introduces $O(L \times K \times Y \times \text{hidden\_nodes}^2)$ operations per time step, where L, K, Y are the input length, kernel size, and output channels, respectively.

The asymptotic analysis reveals that the framework's complexity aligns with the advanced hybrid models, e.g., variational mode decomposition (VMD)-PSO-deep belief network (DBN) (Li et al., 2021), FS-genetic algorithm (GA)-SVR (Zheng et al., 2023). Compared with the benchmark models in the experimental section of this study, such as ELM and BPNN, FS-CDO-CNN-LSTM&SVR still has an advantage in terms of complexity, where $O_{ELM} \approx O(L^3 + L^2 \times n)$ and $O_{BPNN} \approx O(\text{num\_epochs} \times \text{time\_steps} \times \text{hidden\_nodes}^2)$. To further enhance real-time feasibility, lightweight strategies such as pruning redundant neurons (reducing hidden_nodes) or quantizing LSTM weights could be applied without sacrificing accuracy. Future work will integrate these optimizations and report empirical training times on edge devices.

4. Data description and feature selection

4.1. Influencing factors

This study selects the Henry Hub natural gas trading price, which has strong market liquidity and significant influence, as a case study to validate the effectiveness of the proposed model. Recent studies have consistently pointed out that highly correlated core influencing factors can help improve the prediction accuracy of energy prices (Wang et al., 2024; Zhang et al., 2025; Bao et al., 2025). However, natural gas prices are influenced by multiple factors, including supply and demand relationships, temperature changes, alternative energy prices (such as crude oil), and geopolitical risks (Zheng et al., 2023). Specifically, long-term trends in natural gas prices are driven by supply and demand, with natural gas inventory levels, production, imports and exports, and consumption having a significant impact on prices (Xing et al., 2024; Yarlagadda et al., 2024). Temperatures are also correlated with natural gas consumption, which indirectly affects natural gas prices (Li et al., 2022). The impact of the price linkage effect of alternative energy sources, such as crude oil as a core substitute, whose price volatility directly affects natural gas pricing (Perifanis and Dagoumas, 2021). Geopolitical risks, such as the Russia-Ukraine conflict, affect gas prices by triggering price volatility through supply chain disruptions, export restrictions and investment uncertainty (Iliyasu et al., 2025). In addition, exchange rate fluctuations (e.g., EUR/USD, USD/JPY) can also have a non-linear impact on gas prices due to the cross-border nature of trading gas futures. Therefore, based on the above discussion and analysis, this study collects data on factors influencing natural gas prices from five dimensions: production, marketing, commodities, U.S. political and economic indicators, and temperature, as shown in Table 2. These data primarily originate from the U.S. Energy Information Administration (https://www.eia.gov) and the U.S. National Oceanic and Atmospheric Administration (https://www.ncdc.noaa.gov). Additionally, geopolitical risk index data is sourced from a website (https://www.matteoiacoviello.com/gpr.htm) (Caldara and Iacoviell, 2022). All data collected in this study are monthly data, spanning the period from January 1997 to December 2022. Approximately 85% of the data (January 1997 to December 2018, totaling 264 data points) is used as the training set, while the remaining 15% of the data (January 2019 to December 2022, totaling 48 data points) is regarded as the test set to validate the prediction model. In this study, the RobustScaler module in Scikit-learn is used to scale the data based on the median and the range of the upper (75%) and lower (25%) quartiles, in order to effectively deal with outliers. And the missing values are supplemented using linear interpolation. Additionally, the natural gas price series within the study period is tested for stationarity, and the Augmented Dickey-Fuller (ADF) test results indicate that the time series is a stationary series at the 5% significance level.

4.2. Feature selection (FS)

As shown in Table 2, there is a broad consensus that natural gas prices are affected by a multitude of factors, which renders the forecasting task a complicated procedure. Therefore, effective variable selection algorithms are essential for accurately predicting natural gas prices. Three widely used feature selection methods: LASSO, GRA and RF are introduced for variable screening, displayed in Table 3.

Specifically, these three methods are first used separately to conduct variable screening for natural gas price, with the related results presented in Table 4. Subsequently, the screened variables are compared and ranked. And then the common variables screened by at least two methods are identified as the important influencing factors, including NGRR, NGI and PNGI. Finally, these variables are utilized in subsequent model construction and forecasting tasks.

Table 2
Statistical characteristics of natural gas prices and related influencing variables.

Factor group	Variables	Acronym	Unit	Min	Max	Average	Std
Production	U.S. total natural gas Underground storage capacity	NGUS	MMcf	7,952,224	9,265,054	8688928.56	467400.23
	U.S. natural gas gross withdrawals	NGGW	MMcf	1,766,603	3,769,193	2450171.32	540029.48
	U.S. crude oil and natural gas rotary rigs in operation	NGRR	Count	250	2017	1161.55	480.39
Marketing	U.S. natural gas imports	NGI	MMcf	174,225	426,534	286141.02	54563.93
	Price of U.S. natural gas imports	PNGI	$/MMcf	1.5	11.99	4.22	2.16
	U.S. natural gas exports	NHE	MMcf	9527	639,074	157629.60	162498.09
	U.S. natural gas total consumption	NGTC	MMcf	344,920	3,591,691	1931746.41	684581.85
Commodities	Cushing, OK crude oil future	CO	$/Barrel	11.31	134.02	57.37	28.32
	Heating oil future	HO	$/Gallon	0.312	4.30	1.74	0.91
Political and economic indicators of U.S.	US dollar index	DI	/	72.17	120.59	92.35	10.97
	Geopolitical risk index	GPR	/	0.95	10.85	2.77	1.16
	EUR/USD exchange rate	EUR-USD	/	0.85	1.5774	1.19	0.16
	USD/JPY exchange rate	USD-JPY	/	76.19	148.71	109.47	14.03
Temperature	Contiguous U.S. minimum temperature	CMINT	°F	−6.09	6.07	0.20	1.90
	Contiguous U.S. maximum temperature	CMAXT	°F	−6.04	7.60	0.30	2.21
	Contiguous U.S. average temperature	CAVGT	°F	−5.90	6.84	0.25	1.97

Table 3
Introductions of LASSO, GRA and RF methods.

Methods	Types of machine learning	Types of feature selection	Parameter values
LASSO	Supervised	Embedded	0.01 (penalty coefficient)
GRA	Unsupervised	Filter	0.5 (discrimination coefficient)
RF	Supervised	Embedded	100 (number of the estimators)

Table 4
Results of feature selection using LASSO, GRA and RF methods.

Methods	NGUS	NGGW	NGRR	NGI	PNGI	MHE	NGTC	CO
GRA	×	×	□	□	×	×	×	×
LASSO	×	×	□	×	□	×	□	×
RF	×	×	□	□	□	×	×	×
Rank	0	1	3	2	2	0	1	0
Methods	**HO**	**DI**	**GPR**	**EUR-USD**	**USD-JPY**	**CMINT**	**CMAXT**	**CAVGT**
GRA	×	□	×	□	□	×	×	×
LASSO	□	×	×	×	×	×	×	×
RF	×	×	□	×	×	□	×	×
Rank	1	1	1	1	1	1	0	0

5. Experiments and analysis

5.1. Performance measures

Six widely recognized metrics are used to evaluate the forecasting performance of both the developed and comparison models, including mean absolute error (MAE), root mean square error (RMSE), normalized mean square error (NMSE), Theil inequality coefficient (TIC) and coefficient of determination (R^2):

$$\mathrm{MAE} = \frac{1}{T}\sum_{t=1}^{T}|y_t - \widehat{y}_t| \tag{26}$$

$$\mathrm{RMSE} = \sqrt{\frac{1}{T}\sum_{t=1}^{T}(y_t - \widehat{y}_t)^2} \tag{27}$$

$$\mathrm{NMSE} = \frac{1}{T}\sum_{t=1}^{T}\frac{(y_t - \widehat{y}_t)^2}{y_t \widehat{y}_t} \tag{28}$$

$$\mathrm{TIC} = \frac{\sqrt{\frac{1}{T}\sum\limits_{t=1}^{T}(y_t - \widehat{y}_t)^2}}{\sqrt{\frac{1}{T}\sum\limits_{t=1}^{T}y_t^2} + \sqrt{\frac{1}{T}\sum\limits_{t=1}^{T}\widehat{y}_t^2}} \tag{29}$$

$$R^2 = 1 - \frac{\sum\limits_{t=1}^{T}(\widehat{y}_t - y_t)^2}{\sum\limits_{t=1}^{T}(y_t - \overline{y})^2} \tag{30}$$

where y_t denotes the t-th actual value, $\widehat{y}_t$ means the t-th predicted value, and $\overline{y}$ is the average value of the data.

5.2. Experimental design

Three experiments are conducted to evaluate the prediction performance of both the comparison models and the proposed FS-CDO-CNN-LSTM&SVR model, providing a comprehensive assessment of the model's forecasting effectiveness. Specifically, Experiment I focuses on highlighting the benefits of the multivariate model by comparing it with the univariate model. Immediately after that, based on the high-performance multivariate prediction models identified in Experiment I, Experiment II is firstly used to select the optimal single model through comparison. It then validates the superiority of the benchmark model by contrasting it with the improved optimal single model. Finally, it comprehensively compares and analyzes the advantages of the designed FS-CDO-CNN-LSTM & SVR model with regard to improving the forecasting effectiveness. Additionally, Experiment III is designed to further compare and analyze the optimization algorithm, CNN and the proposed combined model to highlight the advantages of the proposed model. More details are presented in the subsequent subsections.

5.3. Experiment I: can multivariate prediction improve prediction accuracy?

Experiment I is designed to test whether multivariate prediction can improve the prediction accuracy by comparing univariate and multivariate models, and to demonstrate the prediction effect of combined variable screening models. It also introduces six single forecasting models commonly used in energy prices prediction, including LSTM, BPNN, ELM, ARIMA, RF and SVR, and utilizes these methods to compare them with their multivariate versions by using FS methods. The forecasting errors of forecasting models in Experiment I are presented in Table 5 and Fig. 2. Based

Table 5
Forecasting errors of forecasting models with univariate and multivariate variables.

Variables	Models	MAE	RMSE	NMSE	TIC	R^2
Univariate	**RF**	0.8310	1.1378	0.3414	0.1409	0.6586
	BPNN	0.6805	1.0743	0.3101	0.1287	0.6899
	ARIMA	0.7375	1.0470	0.2945	0.1306	0.7055
	ELM	0.7039	1.0229	0.2812	0.1235	0.7188
	SVR	0.6967	1.0373	0.2891	0.1236	0.7109
	LSTM	0.6930	1.0215	0.2804	0.1221	0.7196
Multivariate	**FS-RF**	0.5919	0.9319	0.2334	0.1107	0.7666
	FS-BPNN	0.5695	0.8391	0.1892	0.1018	0.8108
	FS-ARIMAX	0.7879	1.0897	0.3191	0.1409	0.6809
	FS-ELM	0.6942	0.9210	0.2279	0.1109	0.7721
	FS-SVR	0.5541	0.7683	0.1586	0.0919	0.8414
	FS-LSTM	0.5330	0.8187	0.1801	0.1008	0.8199

on the results of Table 5 and Fig. 2, the related analysis and discussions can be centered on the following three aspects:

(1) In the comparison of six univariate benchmark models, LSTM and SVR are noted for demonstrating superior prediction levels in natural gas price forecasting. As the results presented in Table 5, both LSTM and SVR outperform other single models in terms of multiple evaluation metrics. For instance, LSTM achieves a MAE of 0.6930 and an R^2 of 0.7196, while SVR atufixZFZcmfiZFZFZTmp[4for 1]ZT'k9fik6HkZAN9fiN.6CZcmp(TpNZFZFZN AF9FF.

models. And the R^2 value of FS-LSTM is

CNN-WOA-LSTM and FS-CNN-CDO-LSTM, consistently outperform the baseline FS-CNN-LSTM model with regard to MAE, RMSE, NMSE, TIC, and

6. Further discussions

In this section, the Diebold-Mariano (DM) test, forecasting effectiveness, the improvements ratio (*IR*) from the proposed model compared with benchmark models, and additional cases for crude oil price forecasting are discussed in this work.

6.1. Hypothesis testing

In this subsection, DM test (Diebold and Mariano, 1995), a well-established statistical hypothesis testing in time series prediction, is adopted to evaluate whether there are significant differences in forecasting performance between the proposed method and each of the benchmark models. Additionally, to further validate the prediction performance, both the forecasting effectiveness (Xiao et al., 2016; Xing et al., 2024) and the variance of forecasting errors (Var_{error}) are calculated, demonstrating the superiority of the developed combined model over the other models. The detailed results are shown in Table 8.

(1) Hypothesis testing is conducted to ascertain if there is a remarkable difference in forecasting performance between the proposed model and the comparison model at a given significance level. From the results presented in Table 8, it is evident that when comparing the proposed model with the univariate model, their DM test values are consistently higher than $Z_{0.10/2} = 1.65$, indicating that significant difference of the prediction performance between the developed model and the univariate model under $\alpha = 0.10$. When comparing with the other multivariate models, it is found that the DM test values are higher than $Z_{0.15/2} = 1.44$ in the vast majority of cases, and more than half of the cases are higher than $Z_{0.10/2} = 1.65$, showing a noticeable difference in forecasting performance when the proposed method is compared with the other benchmark models. Furthermore, based on the experimental results presented in Section 5, it is evident that the combined model in this study achieves highly accurate natural gas price predictions.

(2) The forecasting effectiveness of the models is used to compare the accuracy of the proposed combined model and other nineteen benchmark models. A higher predictive validity score indicates better predictive performance of the model. As shown in Table 8, the forecasting effectiveness values of the univariate models are lower than those of the multivariate models. While there are variations in the forecasting effectiveness across the different models, the proposed combined model consistently achieves the highest value. This suggests that the proposed model offers superior predictive accuracy and outperforms all other comparative models.

(3) The robustness of the model's forecasting performance is assessed by introducing the variance of forecasting errors. According to the results in Table 8, the variance of prediction errors for the univariate model is relatively larger, exceeding 1.0. In contrast, the multivariate model exhibits a smaller variance, although there is a noticeable difference in error variance between different models. Overall, the proposed method shows the smallest error variance of 0.3547, indicating that it possesses the optimal predictive robustness and stability among the twenty models.

Table 8
Results for the DM test and the forecasting effectiveness of forecasting models.

Variables	Models	DM test	FE-1	FE-2	Var_{error}
Univariate	**RF**	−1.8424	0.8258	0.6981	1.0914
	SVR	−1.6916	0.8186	0.6921	1.0932
	LSTM	−1.7590	0.8202	0.6971	1.0626
	ELM	−1.6584	0.8169	0.6763	1.0608
	ARIMA	−2.9310	0.8221	0.7262	1.0817
	BPNN	−1.6030	0.8347	0.7049	1.1785
Multivariate	**FS-RF**	−1.1860	0.8523	0.7404	0.8831
	FS-SVR	−1.7271	0.8592	0.7720	0.5956
	FS-LSTM	−1.6772	0.8766	0.7937	0.6662
	FS-ELM	−2.8416	0.7985	0.6698	0.8606
	FS-ARIMAX	−3.2522	0.8181	0.7369	0.9276
	FS-BPNN	−1.4148	0.8534	0.7542	0.7181
	FS-CDO-LSTM	−1.4410	0.8487	0.7077	0.4441
	FS-CDO-CNN-LSTM	−1.2950	0.8448	0.7034	0.3922
	FS-CNN-LSTM	−2.1727	0.8161	0.6569	0.4610
	FS-PSO-CNN-LSTM	−2.0508	0.8165	0.6561	0.4779
	FS-SSA-CNN-LSTM	−1.7441	0.8359	0.6987	0.4656
	FS-GWO-CNN-LSTM	−1.3866	0.8428	0.7077	0.4554
	FS-WOA-CNN-LSTM	−1.6022	0.8471	0.7350	0.4992
	FS-CDO-CNN-LSTM SVR	–	0.9014	0.8043	0.3547

6.2. Improvement ratio (IR) of the proposed model compared to comparison models

The improvement rate (*IR*) (Xing et al., 2022) metric is constructed to determine whether the proposed model has improved in terms of prediction accuracy compared to the other models.

$$IR_{Index} = \left| \frac{Index_{\text{comparsion}} - Index_{\text{proposed}}}{Index_{\text{comparison}}} \right| \times 100\% \tag{31}$$

where IR_{Index} is an improvement ratio from the proposed model compared to the benchmark methods, *Index* represents the model performance measure, including the MAE, RMSE, NMSE, TIC and R^2.

Within this subsection, the effectiveness of the proposed combined forecasting model is evaluated by means of comparing it with several benchmark models, including RF, SVR, LSTM, ELM, ARIMA, and BPNN. The evaluation is based on the improvement ratio across five model performance metrics. The *IR* results of the proposed model relative to the benchmark model are presented in Table 9. From these results, it is evident that the developed model significantly outperforms the benchmark models in forecasting performance. The more detailed analysis is provided as below.

(1) Although the prediction performance of each univariate model varies, the *IR* values presented in Table 9 are consistently high across all models, such as IR_{NMSE} values greater than 65%. This not only reflects the superior forecasting effectiveness of the proposed model compared with the univariate model, but also points out the deficiency of the univariate forecasting methods in predicting natural gas price without considering the data of influencing factors. It further indicates that future research should pay more attention to the innovation of introducing multivariate data and multivariate models.

(2) For multivariate models, the *IR* values in Table 9 are generally lower than those of corresponding univariate models, reflecting that multivariate comparison models outperform univariate comparison methods in predictive performance. For instance, the IR_{R^2} values of the developed model with respect to RF and FS-RF are 37.0027% and 17.7015%, respectively. In addition, compared to single models and their multivariate versions, hybrid models considering CNN layer and optimization algorithms exhibit lower *IR* values. This

not only highlights the limitations of single models but also underscores the advantage of hybrid models, further validating the scientific credibility and effectiveness of the proposed forecasting model.

In comprehensive comparisons, regardless of univariate or multivariate models, the corresponding IR_{MAE}, IR_{RMSE}, IR_{NMSE} and IR_{TIC} values of the proposed model are basically greater than 20%, and the corresponding IR_{R^2} values are greater than 5%, revealing the superior predictive performance of the presented combined forecasting approach. Based on the experimental results and discussions in Section 5, along with the IR analysis in this section, it is evident that the proposed model outperforms the nineteen comparison models in terms of prediction accuracy.

6.3. Robustness test

To further validate the generalizability of the proposed model, this subsection introduces monthly WTI crude oil price dataset from January 2000 to December 2022 for validation. Based on the relevant references (Xu et al., 2025; Jin and Xu, 2024), the three core influencing factor variables of silver price, EUR/USD, and Henry Hub natural gas price are screened out. Table 10 shows the prediction results of different models on the WTI crude oil dataset. From the results in Table 10, it can be seen that the proposed FS-CDO-CNN-LSTM&SVR model performs best on the WTI crude oil dataset, with the lowest MAE (5.8096), lowest (RMSE (7.8838), lowest NMSE (0.1139), TIC (0.0572), and highest R^2 (0.8879). This indicates that the proposed model can effectively capture the complex patterns of WTI crude oil price fluctuations, demonstrating strong generalization ability. Notably, models using ensemble optimization algorithms such as SSA, WOA, and CDO consistently outperform the baseline FS-CNN-LSTM model, suggesting that these algorithms enhance the predictive performance of the model. The TIC values, which measure the extent of prediction bias relative to actual data, also confirm the stability of models using optimization algorithms. The relatively high R^2 values also indicate that the proposed model possesses strong explanatory power, even when applied to different energy commodities. This robustness may stem from the feature selection (FS) mechanism and the hybrid architecture's ability to effectively capture the nonlinear characteristics of energy prices. In summary, the stable performance across different energy datasets confirms the robustness of the proposed framework, providing a reference for other energy price market predictions.

capabilities in natural gas price prediction and significantly improves prediction accuracy. Specifically, on the one hand, compared to single models with univariate inputs, single models that consider multiple factors exhibit higher prediction accuracy, showing the importance of multivariate data in improving the performance of natural gas price prediction. On the other hand, optimization algorithms and CNNs can significantly improve the prediction performance of standalone LSTM models. By integrating optimization techniques and CNN layers into hybrid LSTM models, the limitations of standalone LSTM models can be addressed, thereby achieving enhanced predictive accuracy. Ultimately, the proposed combined model outperforms other hybrid models in natural gas price forecasting. This superiority and robustness are further confirmed through hypothesis testing, forecasting effectiveness analysis, and improvement ratio assessments.

In summary, the developed combined forecasting model for natural gas price demonstrates both high prediction accuracy and robustness, while also serving as a valuable reference for time series forecasting in other energy price domains. In future research, we will conduct in-depth studies on energy price forecasting and actively incorporate cutting-edge forecasting techniques to further enhance prediction accuracy.

CRediT authorship contribution statement

Pei Du: Writing – review & editing, Writing – original draft, Software, Investigation, Conceptualization. **Xuan-Kai Zhang:** Writing – original draft, Visualization, Software, Data curation. **Jun-Tao Du:** Writing – review & editing, Validation, Supervision, Project administration. **Jian-Zhou Wang:** Writing – review & editing, Supervision, Formal analysis.

Declaration of competing interest

The authors declare that they have no known competing financial interests or personal relationships that could have appeared to influence the work reported in this paper.

Acknowledgments

This study was supported by the funding from the Humanities and Social Science Fund of Ministry of Education of China (No. 22YJCZH028), National Natural Science Foundation of China (Grant No. 72303001), Fundamental Research Funds for the Central Universities (No. JUSRP124043), Anhui Provincial Excellent Young Scientists Fund for Universities (No. 2024AH030001), Anhui Education Department Excellent Young Teachers Fund (No. YQYB2024021) and Basic Research Program of Jiangsu (No. BK20251593).

References

Ali, M., Prasad, R., Xiang, Y., Jamei, M., Yaseen, Z.M., 2023. Ensemble robust local mean decomposition integrated with random forest for short-term significant wave height forecasting. Renew. Energy 205, 731–746. https://doi.org/10.1016/j.renene.2023.01.108.

Bao, H., Hong, Y., Sun, Y., Wang, S., 2025. A novel hybrid nonlinear forecasting model for interval-valued gas prices. J. Forecast. 44 (5), 1826–1848. https://doi.org/10.1002/for.3272.

Behrens, C., Pierdzioch, C., Risse, M., 2018. Testing the optimality of inflation forecasts under flexible loss with random forests. Econ. Modell. 72, 270–277. https://doi.org/10.1016/j.econmod.2018.02.004.

Biau, G., 2012. Analysis of a random forests model. J. Mach. Learn. Res. 13, 1063–1095. https://dl.acm.org/doi/10.5555/2188385.2343682.

Breiman, L., 2001. Random forests. Mach. Learn. 45, 5–32. https://doi.org/10.1023/A:1010933404324.

Cabello-López, T., Carranza-García, M., Riquelme, J.C., García-Gutiérrez, J., 2023. Forecasting solar energy production in Spain: a comparison of univariate and multivariate models at the national level. Appl. Energy 350, 121645. https://doi.org/10.1016/j.apenergy.2023.121645.

Caldara, D., Iacoviell, M., 2022. Measuring geopolitical risk. Am. Econ. Rev. 112 (4), 1194–1225. https://doi.org/10.1257/aer.20191823.

Čeperić, E., Žiković, S., Čeperić, V., 2017. Short-term forecasting of natural gas prices using machine learning and feature selection algorithms. Energy 140, 893–900. https://doi.org/10.1016/j.energy.2017.09.026.

Chapelle, O., Haffner, P., Vapnik, V.N., 1999. Support vector machines for histogram-based image classification. IEEE Trans. Neural Network. 10, 1055–1064. https://doi.org/10.1109/72.788646

Niu, X., Wang, J., Zhang, L., 2022. Carbon price forecasting system based on error correction and divide-conquer strategies. Appl. Soft Comput. 118, 107935. https://doi.org/10.1016/j.asoc.2021.107935.

Park, H.J., Kim, Y., Kim, H.Y., 2022. Stock market forecasting using a multi-task approach integrating long short-term memory and the random forest framework. Appl. Soft Comput. 114, 108106. https://doi.org/10.1016/j.asoc.2021.108106.

Perifanis, T., Dagoumas, A., 2021. Crude oil price determinants and multi-sectoral effects: a review. Energy sources. Energy Sources B Energy Econ. Plann. 16, 787–860. https://doi.org/10.1080/15567249.2021.1922956.

Prasad, R., Ali, M., Kwan, P., Khan, H., 2019. Designing a multi-stage multivariate empirical mode decomposition coupled with ant colony optimization and random forest model to forecast monthly solar radiation. Appl. Energy 236, 778–792. https://doi.org/10.1016/j.apenergy.2018.12.034.

Shehadeh, H.A., 2023. Chernobyl disaster optimizer (CDO): a novel meta-heuristic method for global optimization. Neural Comput. Appl. 35, 10733–10749. https://doi.org/10.1007/s00521-023-08261-1.

Shi, X., Shen, Y., 2021. Macroeconomic uncertainty and natural gas prices: revisiting the Asian Premium. Energy Econ. 94, 105081. https://doi.org/10.1016/j.eneco.2020.105081.

Shi, H., Wei, A., Xu, X., Zhu, Y., Hu, H., Tang, S., 2024. A CNN-LSTM based deep learning model with high accuracy and robustness for carbon price forecasting: a case of Shenzhen's carbon market in China. J. Environ. Manag. 352, 120131. https://doi.org/10.1016/j.jenvman.2024.120131.

Su, M., Zhang, Z., Zhu, Y., Zha, D., 2019. Data-driven natural gas spot price forecasting with least squares regression boosting algorithm. Energies 12 (6), 1094. https://doi.org/10.3390/en12061094.

Sun, S., Jin, F., Li, H., Li, Y., 2021. A new hybrid optimization ensemble learning approach for carbon price forecasting. Appl. Math. Model. 97, 182–205. https://doi.org/10.1016/j.apm.2021.03.020.

Tian, G., Peng, Y., Meng, Y., 2023. Forecasting crude oil prices in the COVID-19 era: can machine learn better? Energy Econ. 125, 106788. https://doi.org/10.1016/j.eneco.2023.106788.

Tibshirani, R., 1996. Regression shrinkage and selection via the lasso. J. Roy. Stat. Soc. B 58 (1), 267–288. https://doi.org/10.1111/j.2517-6161.1996.tb02080.x.

Wang, J., Du, P., Niu, T., Yang, W., 2017. A novel hybrid system based on a new proposed algorithm—Multi-objective whale optimization algorithm for wind speed forecasting. Appl. Energy 208, 344–360. https://doi.org/10.1016/j.apenergy.2017.10.031.

Wang, J., Cao, J., Yuan, S., Cheng, M., 2021. Short-term forecasting of natural gas prices by using a novel hybrid method based on a combination of the CEEMDAN-SE-and the PSO-ALS-optimized GRU network. Energy 233, 121082. https://doi.org/10.1016/j.energy.2021.121082.

Wang, L., Wang, X., Liang, C., 2024. Natural gas volatility prediction via a novel combination of GARCH-MIDAS and one-class SVM. Q. Rev. Econ. Finance 98, 101927. https://doi.org/10.1016/j.qref.2024.101927.

Wu, C., Wang, J., Hao, Y., 2022. Deterministic and uncertainty crude oil price forecasting based on outlier detection and modified multi-objective optimization algorithm. Resour. Policy 77, 102780. https://doi.org/10.1016/j.resourpol.2022.102780.

Xia, X., Li, A., 2024. Global Natural Gas Market and Changing Trends of Natural Gas Trade. In: China International United Petroleum & Chemicals Co., Ltd., Chinese Academy of Social Sciences, Peking University (eds) Annual Report on China's Petroleum, Gas and New Energy Industry (2022–2023). Current Chinese Economic Report Series. Springer, Singapore. https://doi.org/10.1007/978-981-99-7289-0_9.

Xian, H., Che, J., 2022. Unified whale optimization algorithm based multi-kernel SVR ensemble learning for wind speed forecasting. Appl. Soft Comput. 130, 109690. https://doi.org/10.1016/j.asoc.2022.109690.

Xiao, L., Shao, W., Wang, C., Zhang, K., Lu, H., 2016. Research and application of a hybrid model based on multi-objective optimization for electrical load forecasting. Appl. Energy 180, 213–233. https://doi.org/10.1016/j.apenergy.2016.07.113.

Xie, G., Jiang, F., Zhang, C., 2023. A secondary decomposition-ensemble methodology for forecasting natural gas prices using multisource data. Resour. Policy 85, 104059. https://doi.org/10.1016/j.resourpol.2023.104059.

Xing, Q., Wang, J., Lu, H., Wang, S., 2022. Research of a novel short-term wind forecasting system based on multi-objective Aquila optimizer for point and interval forecast. Energy Convers. Manag. 263, 115583. https://doi.org/10.1016/j.enconman.2022.115583.

Xing, Q., Huang, X., Wang, J., Wang, S., 2024. A novel multivariate combined power load forecasting system based on feature selection and multi-objective intelligent optimization. Expert Syst. Appl. 244, 122970. https://doi.org/10.1016/j.eswa.2023.122970.

Xu, Y., Liu, T., Fang, Q., Du, P., Wang, J., 2025. Crude oil price forecasting with multivariate selection, machine learning, and a nonlinear combination strategy. Eng. Appl. Artif. Intell. 139, 109510. https://doi.org/10.1016/j.engappai.2024.1095102.

Yang, L., Gao, T., Lu, Y., Duan, J., Liu, T., 2023a. Neural network stochastic differential equation models with applications to financial data forecasting. Appl. Math. Model. 115, 279–299. https://doi.org/10.1016/j.apm.2022.11.001.

Yang, W., Hao, M., Hao, Y., 2023b. Innovative ensemble system based on mixed frequency modeling for wind speed point and interval forecasting. Inf. Sci. 622, 560–586. https://doi.org/10.1016/j.ins.2022.11.145.

Yao, Z., Wang, Z., Wang, D., Wu, J., Chen, L., 2023. An ensemble CNN-LSTM and GRU adaptive weighting model based improved sparrow search algorithm for predicting runoff using historical meteorological and runoff data as input. J. Hydrol. 625 (A), 129977. https://doi.org/10.1016/j.jhydrol.2023.129977.

Yarlagadda, B., Iyer, G., Binsted, M., Patel, P., Wise, M., McLeod, J., 2024. The future evolution of global natural gas trade. iScience 27 (2), 108902. https://doi.org/10.1016/j.isci.2024.108902.

Zhang, Y., Yao, X., Wu, Q., Huang, Y., Zhou, Z., Yang, J., Liu, X., 2021. Turbidity prediction of lake-type raw water using random forest model based on meteorological data: a case study of Tai lake, China. J. Environ. Manag. 290, 112657. https://doi.org/10.1016/j.jenvman.2021.112657.

Zhang, S., Wu, H., Wang, J., Du, L., 2025. Hybrid deep learning for gas price prediction using multi-factor and temporal features. IEEE Access 13, 11989–12001. https://doi.org/10.1109/ACCESS.2024.3525128.

Zheng, Y., Luo, J., Chen, J., Chen, Z., Shang, P., 2023. Natural gas spot price prediction research under the background of Russia-Ukraine conflict - based on FS-GA-SVR hybrid model. J. Environ. Manag. 344, 118446. https://doi.org/10.1016/j.jenvman.2023.118446.

Ziel, F., Weron, R., 2018. Day-ahead electricity price forecasting with high-dimensional structures: univariate vs. multivariate modeling frameworks. Energy Econ. 70, 396–420. https://doi.org/10.1016/j.eneco.2017.12.016.